Thermodynamic properties of the *XXZ* model in a transverse field

M. Siahatgar
Physics Department, Sharif University of Technology, Tehran 11155-9161, Iran

A. Langari*
Physics Department, Sharif University of Technology, Tehran 11155-9161, Iran
and Institute for Studies in Theoretical Physics and Mathematics, Tehran 19395-5531, Iran
(Received 2 August 2007; revised manuscript received 31 August 2007; published 27 February 2008)

We have numerically studied the thermodynamic properties of the spin $\frac{1}{2}$ *XXZ* chain in the presence of a transverse (noncommuting) magnetic field. The thermal, field dependence of specific heat and correlation functions for chains up to 20 sites has been calculated. The area where the specific heat decays exponentially is considered as a measure of the energy gap. We have also obtained the exchange interaction between chains in a bulk material using the random phase approximation and derived the phase diagram of the three-dimensional material with this approximation. The behavior of the structure factor at different momenta verifies the antiferromagnetic long-range order in the *y* direction for the three-dimensional case. Moreover, we have concluded that the low temperature Lanczos results [M. Aichhorn *et al.*, Phys. Rev. B **67**, 161103(R) (2003)] are more accurate for low temperatures and closer to the full diagonalization ones than the results of finite temperature Lanczos method [J. Jaklic and P. Prelovsek, Phys. Rev. B **49**, 5065 (1994)].

DOI: 10.1103/PhysRevB.77.054435 PACS number(s): 75.10.Jm, 75.40.Cx, 75.40.Mg

I. INTRODUCTION

Quantum phase transition in strongly correlated electron systems, which is the qualitative change in the ground state properties versus a parameter in the Hamiltonian (a magnetic field, amount of disorder,…), has been the focus of research recently.[1,2] Specially, field induced effects in the low dimensional quantum spin models have been attracting much interest from theoretical and experimental points of view in recent years.[3–12] The magnetic properties of a system with axial anisotropy depend on the direction of the applied field. For instance, the magnetic properties of the antiferromagnetic one-dimensional spin 1/2 *XXZ* chain in the longitudinal field are quite different from those in the case of transverse field. The longitudinal field commutes with the rest of the Hamiltonian and preserves the integrability of the model by Bethe ansatz, while a transverse field does not commute and the model is no longer integrable. The transverse field induces the antiferromagnetic long-range order in perpendicular direction to the field and causes a quantum phase transition to the paramagnetic phase at the critical point. Experimental observations[5,6] justify this effect in the quasi-one-dimensional compound, Cs_2CoCl_4.

The qualitative change in the ground state at the quantum critical point (QCP) for zero temperature ($T=0$) affects the finite temperature properties of the model close to the QCP. The quantum critical properties of the Ising model in transverse field have been extensively studied with different approaches.[1,13] However, there is no work on the finite temperature properties of the *XXZ* model in the presence of a transverse field. It is our aim to study the thermodynamic behavior of the anisotropic Heisenberg chain in a transverse field, which is the model Hamiltonian for the mentioned behavior. The Hamiltonian for this system can be written as

$$\mathcal{H} = J\sum_{i=1}^{N} (s_i^x s_{i+1}^x + s_i^y s_{i+1}^y + \Delta s_i^z s_{i+1}^z - h s_i^x), \tag{1}$$

where $J>0$ is the exchange coupling, $0\leq\Delta\leq 1$ is the anisotropy in the z direction, h is proportional to the transverse magnetic field, and s_i^α is the α component of Pauli matrices at site i. Experiments[14] showed that Cs_2CoCl_4 is a realization of this model with $J=0.23$ meV and $\Delta=0.25$.

We will shortly discuss the different approaches to finite temperature properties of the lattice model using the Lanczos method in the next section. We then implement an appropriate approach to get the thermodynamic properties of the *XXZ* model in the transverse field. In this paper, we have studied the finite temperature properties of a chain with $N=20$ sites in magnetic fields $h=0,\ldots,5$ and with anisotropies $\Delta=0$ and $\Delta=0.25$.

II. FINITE TEMPERATURE LANCZOS METHOD

The Lanczos diagonalization method is a powerful numerical tool to study the properties of the quantum many body systems on finite clusters. It is usually used to get the ground state of a quantum model with high accuracy. However, this technique can be extended to finite temperature,[15,16] where one can study the energy spectrum of the system and its behavior under changing system parameters such as anisotropy and magnetic field.

In the Lanczos algorithm, the ground state can be obtained with very high accuracy. However, to get a finite temperature behavior, we need to take the average over the whole Hilbert space (L) with Boltzmann weights, i.e.,

$$\langle\mathcal{O}\rangle = \frac{1}{\mathcal{Z}}\sum_{n}^{L}\langle n|\mathcal{O}e^{-\beta\mathcal{H}}|n\rangle, \quad \mathcal{Z} = \sum_{n}^{L}\langle n|e^{-\beta\mathcal{H}}|n\rangle. \tag{2}$$

It has been proposed that the Lanczos procedure can be used to get a reliable approximation for the finite temperature ($T \neq 0$) properties of the lattice models.[15] In this approach, the Hilbert space is partially spanned by different random initial vectors for several Lanczos procedures. This approach is called finite temperature Lanczos method (FTLM),[15] which is based on the following equations:

$$\langle \mathcal{O} \rangle \simeq \frac{1}{\mathcal{Z}} \sum_{r}^{R} \sum_{m}^{M} e^{-\beta \varepsilon_m^{(r)}} \langle r | \Psi_m^{(r)} \rangle \langle \Psi_m^{(r)} | \mathcal{O} | r \rangle, \tag{3}$$

$$\mathcal{Z} \simeq \sum_{r}^{R} \sum_{m}^{M} e^{-\beta \varepsilon_m^{(r)}} |\langle r | \Psi_m^{(r)} \rangle|^2, \tag{4}$$

where $\beta = 1/k_B T$ ($k_B = 1$) is the Boltzmann constant and $R \sim 10$ is the total number of random samples with different initial vectors $|r\rangle$. The eigenvectors and the corresponding eigenvalues of the tridiagonal matrix are $|\Psi_m^{(r)}\rangle$ and $\varepsilon_m^{(r)}$, respectively, for $m = 1, \ldots, M$. The FTLM procedure works well for finite temperatures; however, it does not converge to the ground state expectation value ($\langle \psi_0 | \mathcal{O} | \psi_0 \rangle$) as $T \to 0$ because of statistical fluctuations, i.e.,

$$\langle \mathcal{O} \rangle = \sum_{r}^{R} \langle \Psi_0 | \mathcal{O} | r \rangle \langle r | \Psi_0 \rangle \Big/ \sum_{r}^{R} \langle \Psi_0 | r \rangle \langle r | \Psi_0 \rangle. \tag{5}$$

This problem can be solved by a symmetric algorithm which is explained below.

A. Low temperature Lanczos method

The low temperature Lanczos method (LTLM) was proposed as a symmetric algorithm to remedy the failure of FTLM at low temperatures.[16] However, LTLM needs more CPU time and memory, but requires fewer steps at low temperatures.[17] LTLM can be formulated similar to the case of FLTM with the following equation:

$$\langle \mathcal{O} \rangle \simeq \frac{1}{\mathcal{Z}} \sum_{r}^{R} \sum_{i,j}^{M} e^{-(1/2)\beta(\varepsilon_i^{(r)} + \varepsilon_j^{(r)})} \langle r | \Psi_i^{(r)} \rangle \langle \Psi_i^{(r)} | \mathcal{O} | \Psi_j^{(r)} \rangle \langle \Psi_j^{(r)} | r \rangle, \tag{6}$$

where the partition function ($\mathcal{Z}$) is calculated in the same way as in Eq. (4). Using this method, as $T \to 0$ we have

$$\langle \mathcal{O} \rangle = \sum_{r}^{R} \langle \Psi_0 | r \rangle \langle r | \Psi_0 \rangle \langle \Psi_0 | \mathcal{O} | \Psi_0 \rangle \Big/ \sum_{r}^{R} \langle \Psi_0 | r \rangle \langle r | \Psi_0 \rangle, \tag{7}$$

which is equal to the ground state expectation value. It is, thus, more accurate to get the low temperature quantum properties.

III. FINITE TEMPERATURE RESULTS

A. Comparison between low temperature Lanczos method and finite temperature Lanczos method

We are interested in the finite temperature properties of the Hamiltonian defined in Eq. (1) and its behavior as $T \to 0$. We have, thus, implemented the LTLM to get the finite temperature properties, which is accurate close to $T = 0$ although it consumes more CPU time and memory. To justify this, we have plotted the x-component spin structure factor at momentum π [$G^{xx}(\pi)$, see Eq. (9)] versus T in Fig. 1. In this figure, we have shown both the FTLM and LTLM results for a chain of length $N = 10$ and 12 together with the exact diagonalization (ED) results for comparison. The discrepancy of FTLM at low temperature ($T \lesssim 0.2$) in comparison with the ED results is clear, especially for $N = 12$ as discussed in the previous section. Figure 1 shows that the LTLM results converge to the ED ones as $T \to 0$ and are in good agreement for higher temperatures.

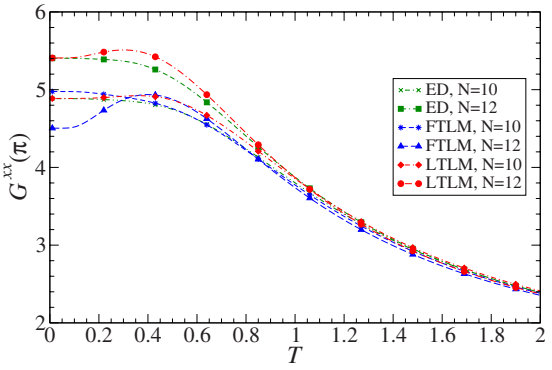

FIG. 1. (Color online) The x-component spin structure factor at momentum π versus temperature for a chain of length $N = 10$ and 12 using FTLM, LTLM, and ED.

B. Specific heat

We have plotted the specific heat of the XXZ chain in the transverse field (h) versus temperature (T) in Fig. 2. The specific heat is computed using

$$C_v = \frac{1}{k_B T^2} (\langle E^2 \rangle - \langle E \rangle^2). \tag{8}$$

The data come from the Lanczos algorithm with random sampling using $R = 100$, $M = 30$–100 (to get eight digits accuracy in the first excited state energy), and for a chain of length $N = 20$ with $\Delta = 0.25$. For $h < h_c \simeq 3.3$, the specific heat shows exponential decay as T goes to zero. This is in agreement with the presence of a finite energy gap in this region. The model is gapless at $h = 0$; however, our data on a finite size do not show this behavior because of the finite size effects. The finite size effects also appear as some level crossing between the first excited state and the ground state in a finite system, which become a degenerate ground state in the thermodynamic limit ($N \to \infty$). This level crossing causes small oscillations close to $T = 0$ and for $h < h_c$. The finite size analysis shows that the gap (E_g) scales as $E_g \sim h^{\nu(\Delta)}$, where $\nu(\Delta = 0.25) = 1.18 \pm 0.01$.[8,9,12] It is the scaling behavior of the second excited state which becomes gapped in the thermodynamic limit ($N \to \infty$). Our data confirm the exponential decay of the specific heat for very low temperatures as $h < h_c$.

However, the general feature—which is the opening of energy gap due to breaking of rotational $U(1)$ symmetry—

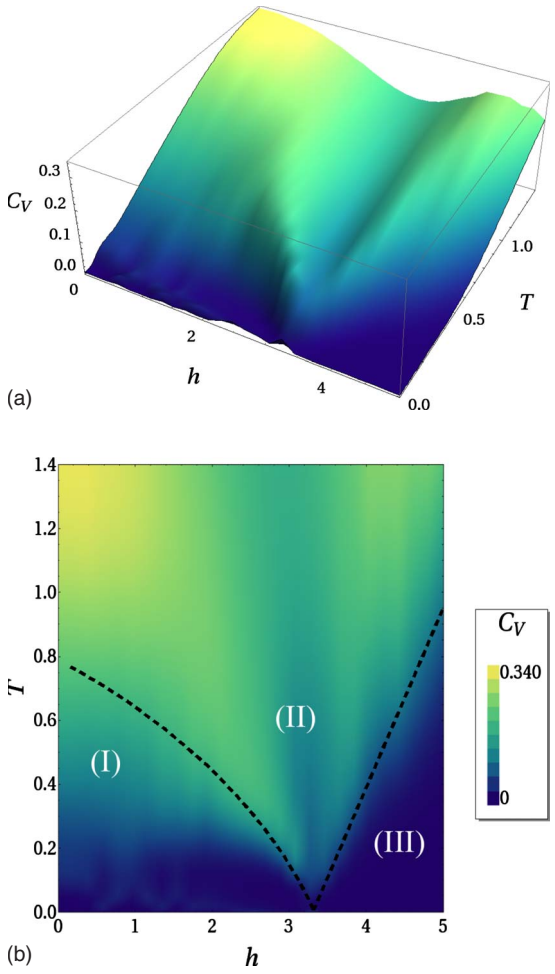

FIG. 2. (Color online) The specific heat of *XXZ* chain in the transverse field (h) versus temperature (T) for $\Delta=0.25$. The data are from LTLM results and $N=20$. (a) The three-dimensional plot. (b) The density plot.

has appeared as the exponential decay of specific heat at low temperatures. The exponential decay vanishes as $h \to h_c$. At the critical point ($h=h_c$), the gap vanishes due to the presence of soft modes which destroy the long-range antiferromagnetic order in the y direction. For $h > h_c$, the system enters the paramagnetic phase and the gap is proportional to $h-h_c$, which is clearly shown in Fig. 2.

Moreover, the density plot in Fig. 2 shows three different regions at finite temperature which are distinguished by different energy scales: (I) the low temperature and $h < h_c$ region, where the classical domain wall quasiparticles define the dynamics of the system;[18] (II) the quantum critical region, where the dynamics is dictated by the quantum fluctuations which become long ranged as both the temporal and spatial correlation lengths diverge; and (III) the low temperature and $h > h_c$ region, where the classical spin flipped quasiparticles represent the dynamical behavior of the model.

Here, we would like to comment on the finite size effects in our calculations. Since the LTLM approach is based on several samplings in the Hilbert space, the finite size effect will be weak and negligible for nonzero temperature. The size dependence of the specific heat is shown in Fig. 3,

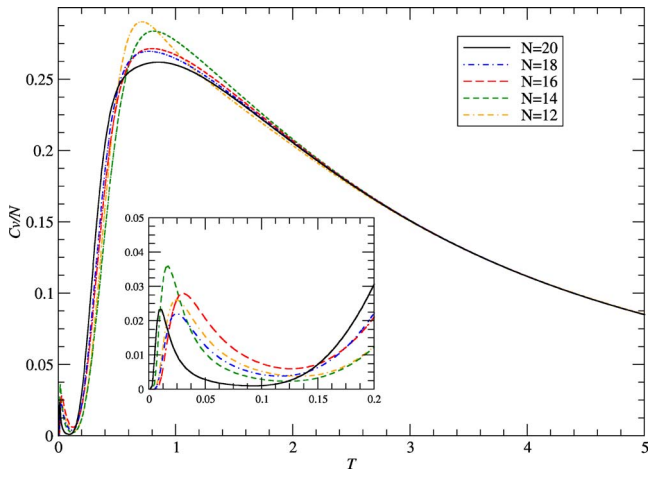

FIG. 3. (Color online) The specific heat of *XXZ* chain versus temperature (T) in the transverse field $h=1$ and $\Delta=0$ for different chain lengths $N=12$, 14, 16, 18, and 20. The inset shows the very low temperature regime.

where different chains with $N=12$, 14, 16, 18, and 20 have been considered. Unless the height of specific heat is not the same for different N, in the low and high temperature regions, all data fall on each other, which justifies the weak finite size effect. We ignore the small size dependence and claim that our data of the specific heat can be interpreted for a very large chain length. The inset of Fig. 3 shows the small oscillations in very low temperature, which are the result of level crossing where the ground state expectation is dominant in the partition function and will vanish as the chain size becomes large.

A remark is in order here. The finite size effect is weak and is compensated by random sampling if the model is not close to a quantum critical point. This is the case of our data presented in Fig. 3 at $h=1$. However, close to quantum critical points, a finite size analysis should be implemented to find the correct behavior. For instance, the level crossing of the first two excited states should be incorporated in a finite size treatment as done in Ref. 12 to find the scaling of energy gap. The situation is more complex when finding the scaling behavior close to h_c since the value of h_c itself is obtained by a finite accuracy, which is an extra source of error in determing the critical exponents.

We have also calculated the specific heat of the *XY* chain, $\Delta=0$, which shows similar qualitative behavior to Fig. 2. It is in agreement with the quantum renormalization group results[11] which state that the universality class of $0<\Delta<1$ is the same as $\Delta=0$ case. However, the critical field h_c is slightly smaller for $\Delta=0$, which is approximately $h_c(\Delta=0) \simeq 3.1$.

C. Static structure factors

We have calculated the static structure factor at finite temperature. The α-component spin structure factor at momentum p is defined by

$$G^{\alpha\alpha}(p) = \sum_{x=1}^{N} \langle s_1^{\alpha} s_{1+x}^{\alpha} \rangle e^{ipx}, \tag{9}$$

where $\langle \ldots \rangle$ is the thermal average defined in Eq. (6).

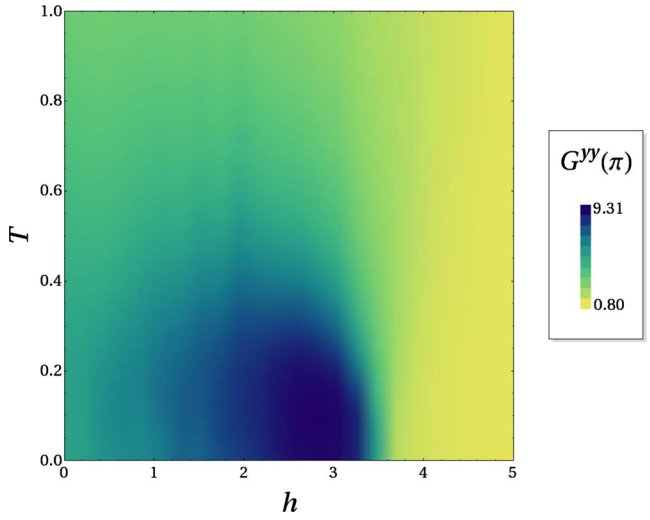

FIG. 4. (Color online) The density plot of y-component spin structure factor at momentum $p=\pi$ versus the transverse magnetic field (h) and temperature (T). The chain length is $N=20$ and $\Delta=0.25$.

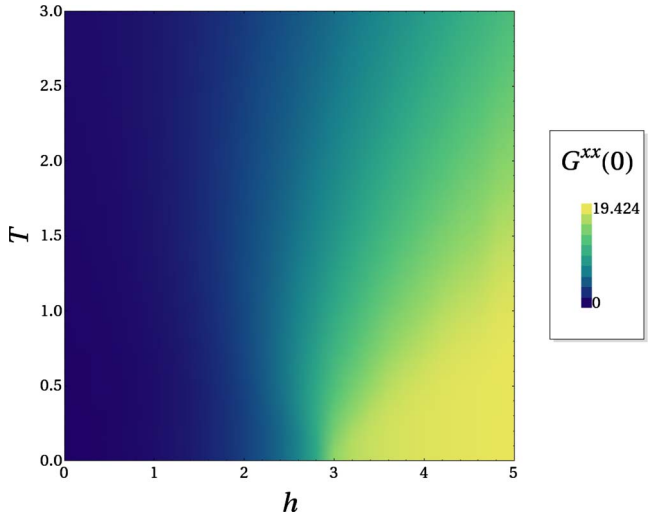

FIG. 5. (Color online) The density plot of x-component spin structure factor at momentum $p=0$ versus the transverse magnetic field (h) and temperature (T). The chain length is $N=20$ and $\Delta=0.25$.

The Hamiltonian [Eq. (1)] is gapless at $h=0$, where there is no long-range ordering in the ground state, while the correlation functions decay algebraically; it is called spin fluid state. The transverse field ($h\neq 0$) breaks the $U(1)$ rotational symmetry to a lower Ising-like symmetry which develops a nonzero energy gap. The ground state then has long-range antiferromagnetic order for $0\leq\Delta<1$. However, due to nonzero projection of the magnetization in the direction of the transverse field, it is a spin-flop phase.

The antiferromagnetic ordering in the y direction for the spin-flop phase implies that the y-component structure factor at $p=\pi$ diverges as the size of the system goes to infinity. This can be seen as a peak in the structure factor.

The density plot of $G^{yy}(\pi)$ is shown in Fig. 4 versus temperature (T) and transverse field (h) for $\Delta=0.25$. The peak in $G^{yy}(\pi)$ (which is a signature of antiferromagnetic ordering) is the dark (blue) area in Fig. 4. It shows that the ordering is absent at $h=0$ and will gradually appear for increasing h. The antiferromagnetic ordering in the y direction can be represented by staggered magnetization in the same direction (sm_y) as the order parameter. Figure 4 shows that sm_y becomes maximum at $h\simeq 2$. The point $h\simeq 2$ can also represent the position where the gap becomes maximum. Further increasing the transverse field suppresses the antiferromagnetic ordering until reaching the critical point $h=h_c$. It is clearly shown in Fig. 4 that sm_y becomes zero at $h=h_c$.

The density plot of the x-component structure factor at $p=0$ has been presented in Fig. 5 versus T and h. The value of $G^{xx}(0)$ is small for $h\lesssim 2$, which implies low alignment of the spins in the direction of the external field. However, this value starts to grow for $h>2$ and obviously saturates for $h\geq h_c=3.3$. The maximum value of $G^{xx}(0)$ is the signature of long-range order in the field direction where the moments saturate at the maximum value in the paramagnetic phase. However, as the temperature increases, the ordering will be washed out due to thermal fluctuations which destroy the long-range order in one dimension. The long-range order at finite temperature is meaningful in the sense of a three-dimensional model which is composed of weakly coupled chains. This will be explained in the next sections via the random phase approximation (RPA).

D. Magnetic susceptibility

Magnetic susceptibility can be calculated using

$$\chi_{1D}^{\alpha}\cong\frac{1}{T}G^{\alpha\alpha}(k). \tag{10}$$

To get the susceptibility of the bulk material, which is composed of coupled chains with interchain exchange, $J_\perp$, we used the RPA. It is a mean field approach where the one-dimensional chain is treated exactly, while the interactions between chains are weak and considered in a mean field approach. In the disordered phase, the dynamical susceptibility of coupled chains at zero frequency is[10]

$$\chi^{yy}(p)=\frac{\chi_{1D}^{yy}(p)}{1-J_\perp\chi_{1D}^{yy}(p)}, \tag{11}$$

where $\chi_{1D}^{yy}(p)$ is the one-dimensional susceptibility in the y direction and momentum p, which comes from the LTLM computations. We have plotted $\chi^{yy}(p=\pi)$ versus temperature in Fig. 6 for different transverse fields. The susceptibility diverges at finite (nonzero) temperature for $h<h_c$, which shows the phase transition from the disordered phase to the antiferromagnetic long-range ordered phase. For $h>h_c$, the susceptibility only diverges at $T=0$, which justifies no long-range order at finite temperature.

We have also used the RPA to calculate the interchain exchange coupling ($J_\perp$) from our numerical computations and experimental data.[5] This can help us to justify the mean field treatment of the interactions between chains. We have

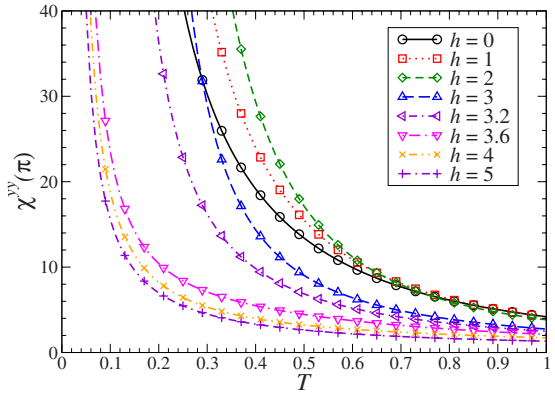

FIG. 6. (Color online) The RPA three-dimensional $\chi^{yy}(\pi)$ versus temperature for different transverse fields, $\Delta=0.25$, and $J_\perp \simeq 0.004\,58J$ for Cs_2CoCl_4. For $h<h_c$, the susceptibility diverges at finite temperature, while for $h>h_c$, it only diverges at $T=0$.

used the $h=0$ and $T_N \simeq 217^{mK} \simeq 0.0813J$ data presented in Refs. 5 and 6 and solved $1-J_\perp \chi^{yy}_{1D}(T_N,\pi)=0$ to find $J_\perp$. The result of this calculation is $J_\perp \simeq 0.004\,58J$, which can be compared with $J_\perp \simeq 0.0147J$ estimated in Ref. 10. The coupling between chains is 2 orders of magnitude smaller than the intrachain interaction, which verifies the RPA implemented here. We then used the value of $J_\perp \simeq 0.004\,58J$ to find the whole phase diagram of the bulk material using our numerical data at finite magnetic field. The phase diagram of the three-dimensional system has been presented in Fig. 7. The phase diagram shows the border between the ordered and disordered phases in the T-h plane. This is in good agreement with the experimental data presented in Fig. 11 of Ref. 5.

E. Summary and discussion

We have implemented the symmetric algorithm of the Lanczos method to find the finite temperature (thermodynamic) properties of the anisotropic Heisenberg model in the presence of a transverse magnetic field. It is argued that the

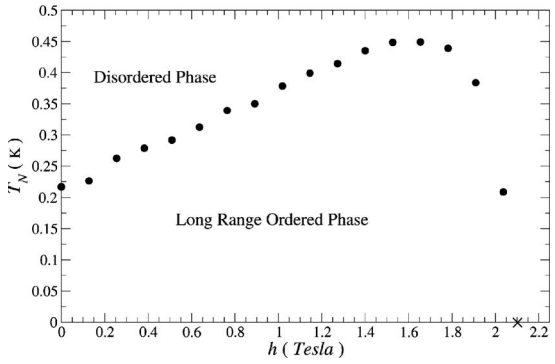

FIG. 7. The phase diagram of the bulk material in T (temperature) and h (magnetic field) planes. It is the result of LTLM for one-dimensional chain and RPA to get the bulk property with interchain exchange coupling $J_\perp \simeq 0.004\,58J$ for Cs_2CoCl_4. The cross ($\times$) represents the zero temperature critical field.

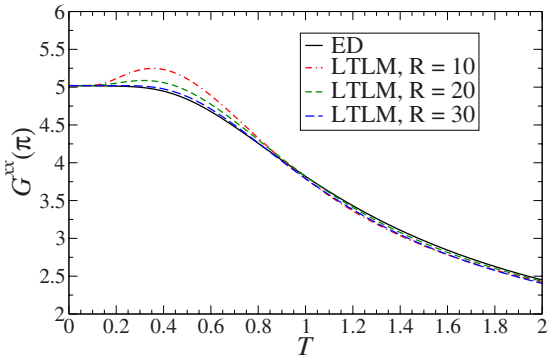

FIG. 8. (Color online) The effect of number of random samples in the x component of spin structure factor at momentum $p=\pi$ versus temperature.

symmetric algorithm[16] (LTLM) is more accurate at low temperatures than the finite temperature Lanczos method.[15] We have found that the specific heat decays exponentially at low temperatures for $h<h_c$, which justifies the presence of finite energy gap in the lowest part of the spectrum. The gap vanishes both at $h=0$ and $h=h_c$, with a maximum around $h=2$. A similar behavior has been observed for the y-component structure factor at the antiferromagnetic wave vector $p=\pi$. It shows that the onset of transverse field opens a gap which stabilizes the antiferromagnetic (AF) order in the y direction. The AF ordering becomes maximum at $h=2$ and starts to decrease by further increasing the magnetic field. The long-range magnetic order vanishes at the critical point ($h=h_c$), where the gap becomes zero and soft modes destroy the ordering. The data of the one-dimensional model can be used within a random phase approximation to find the phase diagram of the experiments[5] done on Cs_2CoCl_4. We have estimated the interchain coupling to be $J_\perp \simeq 0.004\,58J$, which justifies the RPA method. Moreover, we have plotted the phase diagram of the three-dimensional model (weakly coupled chains) in Fig. 7, which is in very good agreement with the experimental results presented in Ref. 5.

We have shown that the LTLM results are not finite size dependent if they are not close to the quantum critical points. It is the result of random sampling which exists in the algorithm. However, a finite size analysis is required to find the

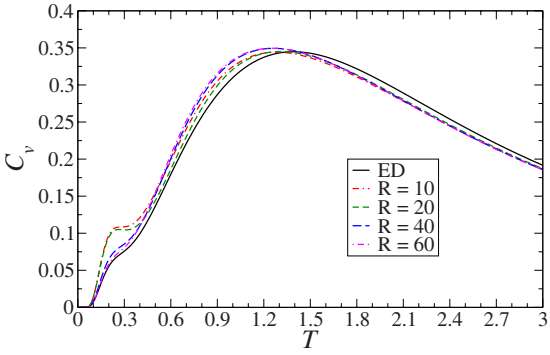

FIG. 9. (Color online) Specific heat vs temperature with different numbers of random samples, with $h=0$ and $\Delta=0.25$. The solid black line is the result of exact diagonalization.

scaling behavior close to quantum critical points. The scaling property of the energy gap has already been discussed in Ref. 12, while there are other aspects which are open for further investigations.

We would also like to comment on the number of random sampling in this method. We have plotted the x-component structure factor at $p=\pi$ versus temperature in Fig. 8 for different samplings, $R=10$, 20, and 30, and the exact diagonalization on the full spectrum. It shows that $R=30$ is enough to get a good accuracy for the finite temperature behavior. Similar data for the specific heat versus temperature and $R=10$, 20, 40, and 60 in Fig. 9 show that the number of $R=60$ sampling reproduces well the exact results. We then conclude that our results are reliable for $R=100$. One should note that the CPU required time is proportional to the number of sampling (R).

ACKNOWLEDGMENTS

The authors would like to thank P. Thalmeier, M. Kohandel, B. Schmidt, and H. Rezania for their valuable comments and discussions. This work was made possible by the facilities of the Shared Hierarchical Academic Research Computing Network (SHARCNET: www.sharcnet.ca). This work was supported in part by the center of excellence in Complex Systems and Condensed Matter (www.cscm.ir).

*langari@sharif.edu; http://spin.cscm.ir

[1] S. Sachdev, *Quantum Phase Transitions* (Cambridge University Press, Cambridge, England, 1999).
[2] M. Vojta, Rep. Prog. Phys. **66**, 2069 (2003).
[3] I. Affleck and M. Oshikawa, Phys. Rev. B **60**, 1038 (1999).
[4] G. Uimin, Y. Kudasov, P. Fulde, and A. Ovchinnikov, Eur. Phys. J. B **16**, 241 (2000).
[5] M. Kenzelmann, R. Coldea, D. A. Tennant, D. Visser, M. Hofmann, P. Smeibidl, and Z. Tylczynski, Phys. Rev. B **65**, 144432 (2002).
[6] T. Radu, Ph.D. thesis, Max Planck Institute for Chemical Physics of Solids, 2002.
[7] M. Kohgi, K. Iwasa, J. M. Mignot, B. Fak, P. Gegenwart, M. Lang, A. Ochiai, H. Aoki, and T. Suzuki, Phys. Rev. Lett. **86**, 2439 (2001).
[8] D. V. Dmitriev, V. Y. Krivnov, A. A. Ovchinnikov, and A. Langari, JETP **95**, 538 (2002).
[9] D. V. Dmitriev, V. Y. Krivnov, and A. A. Ovchinnikov, Phys. Rev. B **65**, 172409 (2002).
[10] D. V. Dmitriev and V. Y. Krivnov, Phys. Rev. B **70**, 144414 (2004).
[11] A. Langari, Phys. Rev. B **69**, 100402(R) (2004).
[12] A. Langari and S. Mahdavifar, Phys. Rev. B **73**, 054410 (2006).
[13] S. Sachdev and A. P. Young, Phys. Rev. Lett. **78**, 2220 (1997).
[14] H. A. Algra, L. J. de Jongh, H. W. J. Blte, W. J. Huiskamp, and R. L. Carlin, Physica B & C **82**, 239 (1976).
[15] J. Jaklič and P. Prelovšek, Phys. Rev. B **49**, 5065 (1994).
[16] M. Aichhorn, M. Daghofer, H. Evertz, and W. von der Linden, Phys. Rev. B **67**, 161103(R) (2003).
[17] M. Siahatgar, M.S. thesis, Sharif University of Technology, 2008.
[18] S. Sachdev and A. P. Young, Phys. Rev. Lett. **78**, 2220 (1997).